Striatal Acetylcholine-Dopamine Imbalance in Parkinson Disease

Sanchez-Catasus, Carlos A.; Bohnen, Nicolaas; D'Cruz, Nicholas; Muller, Martijn L. T. M.

Published in:
Journal of Nuclear Medicine

DOI:
10.2967/jnumed.121.261939

Publication date:
2022

Striatal Acetylcholine–Dopamine Imbalance in Parkinson Disease: In Vivo Neuroimaging Study with Dual-Tracer PET and Dopaminergic PET–Informed Correlational Tractography

Carlos A. Sanchez-Catasus[1–3], Nicolaas I. Bohnen[1,3–5], Nicholas D'Cruz[6], and Martijn L.T.M. Müller[1,3]

[1]Division of Nuclear Medicine, Department of Radiology, University of Michigan Health System, Ann Arbor, Michigan; [2]Department of Nuclear Medicine and Molecular Imaging, University Medical Center Groningen, Groningen, The Netherlands; [3]Morris K. Udall Center of Excellence for Parkinson's Disease Research, University of Michigan, Ann Arbor, Michigan; [4]Department of Neurology, University of Michigan Health System, Ann Arbor, Michigan; [5]Neurology Service and GRECC, Veterans Administration Ann Arbor Healthcare System, Ann Arbor, Michigan; and [6]Department of Rehabilitation Sciences, KU Leuven, Leuven, Belgium

Previous studies of animal models of Parkinson disease (PD) suggest an imbalance between striatal acetylcholine and dopamine, although other studies have questioned this. To our knowledge, there are no previous in vivo neuroimaging studies examining striatal acetylcholine–dopamine imbalance in PD patients. Using cholinergic and dopaminergic PET (^{18}F-fluoroethoxybenzovesamicol [^{18}F-FEOBV] and ^{11}C-dihydrotetrabenazine [^{11}C-DTBZ], respectively) and correlational tractography, our aim was to investigate the acetylcholine–dopamine interaction at 2 levels of dopaminergic loss in PD subjects: integrity loss of the nigrostriatal dopaminergic white matter tract and loss at the presynaptic-terminal level. **Methods:** The study involved 45 subjects with mild to moderate PD (36 men, 9 women; mean age, 66.3 ± 6.3 y, disease duration, 5.8 ± 3.6 y; Hoehn and Yahr stage, 2.2 ± 0.6) and 15 control subjects (9 men, 6 women; mean age, 69.1 ± 8.6 y). PET imaging was performed using standard protocols. We first estimated the integrity of the dopaminergic nigrostriatal white matter tracts in PD subjects by incorporating molecular information from striatal ^{11}C-DTBZ PET into the fiber tracking process using correlational tractography (based on quantitative anisotropy [QA], a measure of tract integrity). Subsequently, we used voxel-based correlation to test the association of the mean QA of the nigrostriatal tract of each cerebral hemisphere with the striatal ^{18}F-FEOBV distribution volume ratio (DVR) in PD subjects. The same analysis was performed for ^{11}C-DTBZ DVR in 12 striatal subregions (presynaptic-terminal level). **Results:** Unlike ^{11}C-DTBZ DVR in striatal subregions, the mean QA of the nigrostriatal tract of the most affected hemisphere showed a negative correlation with a striatal cluster of ^{18}F-FEOBV DVR in PD subjects (corrected $P = 0.039$). We also found that the mean ^{18}F-FEOBV DVR within this cluster was higher in the PD group than in the control group ($P = 0.01$). Cross-validation analyses confirmed these findings. We also found an increase in bradykinesia ratings associated with increased acetylcholine–dopamine imbalance in the most affected hemisphere ($r = 0.41$, $P = 0.006$). **Conclusion:** Our results provide evidence for the existence of striatal acetylcholine–dopamine imbalance in early PD and may provide an avenue for testing in vivo effects of therapeutic strategies aimed at restoring striatal acetylcholine–dopamine balance in PD.

Key Words: Parkinson disease; acetylcholine–dopamine imbalance; dopaminergic nigrostriatal connectivity; ^{18}F-FEOBV PET; ^{11}C-DTBZ PET

Received Jan. 13, 2021; revision accepted May 27, 2021.

For correspondence or reprints, contact Martijn L.T.M. Müller (mmuller@c-path.org).

Published online Jul. 16, 2021.

J Nucl Med 2022; 63:438–445
DOI: 10.2967/jnumed.121.261939

Striatal cholinergic interneurons are the main source of cholinergic innervation in the striatum (*1*,*2*). Although these interneurons represent a small percentage of all striatal neurons, they are distributed throughout the striatum and their presynaptic terminals overlap with dopaminergic axonal projections originating in the substantia nigra pars compacta (*2*). A prevailing view is that the acetylcholine and dopamine signaling systems must be in dynamic balance in the striatum for optimal movement control (*3*,*4*).

Parkinson disease (PD) is a neurodegenerative movement disorder characterized by nigrostriatal dopaminergic losses (*5*,*6*). These losses may result in a striatal acetylcholine–dopamine imbalance (*3*), at least in the early disease stages. Although several animal model studies support this concept (*7–9*), other studies have questioned the acetylcholine–dopamine imbalance model (*10–12*). For example, Herrera-Marschitz et al. found that striatal acetylcholine levels were not modified by unilateral dopaminergic deafferentation in a rat model (*10*). In a subsequent study, they suggested that striatal dopamine and acetylcholine release is modulated by independent mechanisms (*11*). A more recent study suggested that striatal dopamine deficiency decreased acetylcholine production and inhibited normal striatal cholinergic interneuron spike timing in Parkinsonian mice (*12*). They also found that acetylcholine decreased to a lesser extent than dopamine, resulting in an increased acetylcholine-to-dopamine ratio (*12*) suggestive of the acetylcholine–dopamine imbalance in PD.

To the best of our knowledge, there are no prior in vivo studies on humans with PD that examine changes in striatal cholinergic interneuron activity in response to nigrostriatal dopaminergic losses. A better understanding of striatal dopaminergic and cholinergic system interaction may have implications for the development of new therapeutic strategies in PD.

^{18}F-fluoroethoxybenzovesamicol (^{18}F-FEOBV) is a PET radioligand that selectively binds to the vesicular acetylcholine transporter and allows for binding quantification in brain regions with high presynaptic cholinergic activity, such as the striatum (*13*). ^{11}C-dihydrotetrabenazine (^{11}C-DTBZ) selectively binds to the vesicular monoamine transporter type 2 and is useful as a marker

of the nigrostriatal dopaminergic presynaptic terminal because of the high specificity in the striatum (*14*). However, like other PET dopaminergic presynaptic markers, ^{11}C-DTBZ may be influenced by pharmacologic compensation or regulation (*15–17*). These processes might obscure the striatal acetylcholine–dopamine interaction at the presynaptic-terminal level; therefore, more robust approaches may be required to capture dopaminergic transmission.

We recently introduced a methodology to estimate dopaminergic nigrostriatal white matter tract integrity (i.e., dopaminergic nigrostriatal connectivity) in subjects with early PD (*18*). This methodology integrates striatal ^{11}C-DTBZ PET information into the fiber-tracking process using diffusion MRI (dMRI)–based correlational tractography. Tract integrity is measured as the mean quantitative anisotropy (QA) across the estimated tract. QA measures the density of anisotropic water diffusion (*19*) and provides a more reliable integrity metric than do standard diffusion measures (*18*,*20*,*21*). Furthermore, the dopaminergic nigrostriatal white matter tract should be less influenced by compensatory mechanisms than is the presynaptic-terminal level.

Using in vivo cholinergic and dopaminergic PET and dopaminergic PET–informed correlational tractography, our aim was to examine the striatal acetylcholine–dopamine imbalance hypothesis in patients with early PD while considering the integrity loss of the nigrostriatal dopaminergic pathway at 2 levels: dopaminergic nigrostriatal connectivity (i.e., loss of mean QA of the nigrostriatal tract) and the presynaptic-terminal level (i.e., loss of striatal ^{11}C-DTBZ binding). We also examined differences in striatal cholinergic binding between PD subjects and healthy controls.

MATERIALS AND METHODS

Subjects

The study included 45 subjects with mild to moderate PD (36 men and 9 women; mean age, 66.3 ± 6.3 y), of whom 30 were previously reported (*18*). The study also included 15 age- and sex-matched healthy control subjects (9 men and 6 women; mean age, 69.1 ± 8.6 y) with available cholinergic ^{18}F-FEOBV PET results.

Similar to our previous report (*18*), selection of PD subjects was based on 3 criteria: first, only subjects with mild to moderate PD (Hoehn and Yahr stage ≤ 3) were included to avoid a floor effect associated with severe nigrostriatal dopaminergic denervation in more advanced stages; second, high-quality dMRI reconstruction had to be available; and third, an interval of no more than 2 months (mo) had to have passed between clinical examinations and neuroimaging assessments to ensure no significant clinical changes. Table 1 summarizes the main demographic and clinical characteristics of all participants.

All patients met the U.K. Parkinson Disease Society Brain Bank clinical diagnostic criteria for PD (*22*) and showed the typical pattern of striatal dopaminergic denervation on ^{11}C-DTBZ PET congruent with this diagnosis (*14*). The Movement Disorder Society revised unified Parkinson disease rating scale examination (*23*), the Hoehn and Yahr scale (*24*), and Montreal cognitive assessment (*25*) were performed on PD subjects for clinical assessments. The motor examination was performed in the dopaminergic medication–off state, except for 2 de novo patients. No subjects were treated with anticholinergic or cholinesterase inhibitor drugs. Motor symptoms were predominantly on the right side of the body in 29 patients and on the left side in the other 16 patients.

The study was approved by the Institutional Review Boards of the University of Michigan School of Medicine and the Veterans Affairs Ann Arbor Health Care System. Written informed consent was obtained from all subjects before any research procedures took place.

Imaging Procedures

We realigned (right to left) image data of the 16 patients with a left predominance of clinical symptoms in order to create a uniform sample, given the asymmetry in early PD for the typical motor symptoms and striatal ^{11}C-DTBZ (*14*). Thus, the left hemisphere represented the clinically most affected (MA) hemisphere in all patients, and the right hemisphere the clinically least affected.

PET Imaging. All subjects underwent both PET scans during the same visit, except for control subjects, on whom dopaminergic PET was not performed. Dynamic PET imaging was performed in 3-dimensional mode using an ECAT Exact HR tomograph (Siemens Molecular Imaging, Inc.). Preprocessing parameters for both PET sets of data can be found in detail elsewhere (*26*,*27*). ^{11}C-DTBZ (555 MBq) and ^{18}F-FEOBV (256 MBq) radioligands were prepared as previously described and injected following standard routines (*28*,*29*). Dopaminergic PET was performed in the dopaminergic-off state, whereas cholinergic PET was performed in the dopaminergic-on state in PD subjects.

For both PET tracers, dynamic frames were spatially coregistered within subjects with a rigid body transformation to reduce the motion effect during the imaging session (*30*). Motion-corrected PET frames were spatially coregistered to high-resolution MR images using SPM12 software (Wellcome Trust Centre for Neuroimaging, https://www.fil.ion.ucl.ac.uk/spm). Distribution volume ratio (DVR) images were then calculated for the 2 PET tracers following previously reported methodologies (*31*,*32*).

For MRI-coregistered ^{11}C-DTBZ DVR images, we manually traced the volumes corresponding to 6 striatal subregions in each brain hemisphere on the MR image following a methodology described previously (*33*). The striatal subregions included the anteroventral striatum, middle caudate, caudate head, ventral putamen, anterior putamen, and posterior putamen. These striatal subregions encompass the typical ventral-to-dorsal and anterior-to-posterior gradient of striatal dopaminergic denervation in early PD (*33*) and were used as striatal dopaminergic variables of interest at the presynaptic-terminal level in the voxel-based correlation analysis with striatal ^{18}F-FEOBV DVR. Supplemental Figure 1 shows the histograms, mean (±SD), median, and range of ^{11}C-DTBZ DVR for these subregions (supplemental materials are available at http://jnm.snmjournals.org). The analysis was also performed with the whole striatum as a variable of interest.

For voxel-based correlation analysis, ^{18}F-FEOBV DVR images were spatially standardized to the Montreal Neurologic Institute space based on the DARTEL (Diffeomorphic Anatomic Registration Through Exponentiated Lie Algebra) procedure (SPM12). DARTEL transformations were estimated on the basis of T1-weighted MR images and subsequently applied to PET images coregistered with the MR images. ^{18}F-FEOBV DVR images of control subjects were transformed in the same way to perform a voxel-based group comparison. Spatially normalized ^{18}F-FEOBV DVR images were smoothed with the SPM12 default gaussian isotropic kernel of 8 mm in full width at half maximum to reduce the anatomic variability between individual brains and enhance the signal-to-noise ratio.

MRI. All subjects underwent high-resolution structural brain MRI (T1-weighted) for anatomic coregistration with the corresponding PET scans. MRI was performed on a 3-T Achieva system (Philips). A detailed description of the structural brain MRI acquisition parameters can be found elsewhere (*26*).

During the same visit, dMRI was performed for dopaminergic PET-informed correlational tractography. The acquisition parameters and preprocessing of the MR images have been described in detail previously (*18*). Quality control of the preprocessed dMRI image data was performed using the DSI Studio toolbox (http://dsi-studio.labsolver.org). The neighboring correlation was high and similar across all dMRI volumes (0.88 ± 0.02), indicating a good quality of preprocessed dMRI data relative to motion artifacts and signal-to-noise ratio.

TABLE 1
Demographic and Clinical Characteristics of PD and Control Subjects

Characteristic	PD (n = 45)	Control (n = 15)	Statistical significance
Age (y)	66.3 ± 6.3	69.1 ± 8.6	t = 1.3; P = 0.19
Sex			χ^2 = 2.4; P = 0.12
Male	36	9	
Female	9	6	
Handedness			χ^2 = 0.25; P = 0.62
Right	41	13	
Left	4	2	
MoCA	27.0 ± 2.6	27.6 ± 1.8	t = 0.87; P = 0.39
MDS-UPDRS			
Part I	5.1 ± 4.5		
Part II	5.5 ± 3.5		
Part III	34.3 ± 13.2		
Bradykinesia subscore*	11.6 ± 5.9		
Tremor subscore*	8.8 ± 4.4		
Rigidity subscore*	7.5 ± 2.9		
PIGD subscore*	2.5 ± 2		
MDS-UPDRS (I–III) total score	44.9 ± 16.8		
Hoehn and Yahr stage	2.2 ± 0.6 (median, 2.5; range, 1–3)		
Disease duration (y)	5.8 ± 3.6		
Levodopa equivalent dose (mg)	636.6 ± 374.5		

*Derived from MDS-UPDRS (part III).
MoCA = Montreal cognitive assessment; MDS-UPDRS = Movement Disorder Society revised unified Parkinson disease rating scale; PIGD = postural instability and gait difficulties.

Dopaminergic PET-Informed Correlational Tractography. Correlational tractography was performed as previously described (*18*) for a larger sample of PD participants. In brief, dMRI preprocessed data in the PD group were reconstructed in the Montreal Neurologic Institute space using q-space diffeomorphic reconstruction (*34*) implemented in the DSI Studio toolbox. Our correlational tractography-based approach first constructs a group-based tract template in each brain hemisphere by tracking QA in white matter fibers that correlate with ^{11}C-DTBZ DVR corresponding to anteroventral striatum to optimally guide tract reconstruction with dopaminergic specificity (*18*). The procedure uses a deterministic fiber tracking (*35*), with the substantia nigra as the seed region and the whole striatum as the terminating region corresponding to each brain hemisphere. In a second step, the mean QA extracted from each subject across the template (from each hemisphere) was used as a measure of the whole-tract integrity at the individual level.

The individual mean QA values of each PD subject in each hemisphere, in the striatal subregions described above, and in the whole striatum were used as dopaminergic variables of interest in the voxel-based correlation analysis with striatal ^{18}F-FEOBV DVR.

Statistical Analysis

Voxel-based correlation analysis was performed using SPM12 to test the association of the mean QA of the dopaminergic nigrostriatal tract or striatal subregional presynaptic-terminal ^{11}C-DTBZ DVR (and the whole striatum) of each hemisphere with striatal ^{18}F-FEOBV DVR in PD subjects. An explicit bilateral mask was used to exclude nonstriatal voxels. Age and sex were modeled as standard nuisance covariates. Positive and negative correlations were tested. The results of this analysis were then used to create a volume of interest (VOI), based on significant clusters, to evaluate the Pearson correlation of the VOI mean values of ^{18}F-FEOBV DVR with the corresponding dopaminergic variables of interest, and for comparison between groups (PD vs. control) within that VOI using the Student t test for independent samples.

In a second analysis, the levodopa equivalent dose and the duration and stage of the disease (defined as a binary variable according to the Hoehn and Yahr scale: mild = 0 for Hoehn and Yahr ≤ 2; moderate = 1 for 2 < Hoehn and Yahr ≤ 3) were considered as additional nuisance covariates to test their possible confounding effects on the first voxel-based correlation analysis.

Since the presence of outliers in the data can affect the correlation analysis, we repeated voxel-based correlation analysis for dopaminergic variables of interest that showed potential outliers. For outlier detection, we used the Grubbs test. In the event that a variable was significant for the Grubbs test and did not have a normal distribution (significant Shapiro–Wilk test; Supplemental Fig. 1), we also used the interquartile rule to find outliers as follows: first, calculation of the interquartile range of the data of each subregion; second, calculation of the lower boundary by subtracting 1.5 × (interquartile range) from the first quartile; and third, calculation of the upper boundary by adding 1.5 × (interquartile range) to the third quartile. Any value outside the upper and lower boundaries was considered a potential outlier.

Additionally, a voxel-based group comparison was performed between the control and PD groups for striatal ^{18}F-FEOBV DVR, controlling for age and sex.

In all SPM analyses, we applied threshold P values of 0.001 (uncorrected) at the voxel level and 0.05 corrected for multiple comparisons at the cluster level by using the familywise error approach.

Cross Validation. To assess the generalizability of our main findings, cross validation was performed using the leave-one-out (LOO) methodology. Since the mean QA of the dopaminergic nigrostriatal tract in the MA hemisphere (Fig. 1A) was the only dopaminergic variable of interest that showed a significant correlation with the striatal ^{18}F-FEOBV DVR, the cross validation was applied to this model (MA-tract model) and to the VOI model derived from the voxel-based correlation analysis (Fig. 1B).

In the MA-tract model, the training set was defined as the mean QA extracted in each PD subject from the group-based tract template in the MA hemisphere. To get the validation element of a single PD subject, we constructed a new tract template that left that specific PD subject out. This new tract template was used to extract the mean QA from that PD subject (mean QA-LOO). This process was repeated for each of the 45 PD subjects.

In the VOI model, the training set was defined as the mean ^{18}F-FEOBV DVR of each PD subject within the VOI based on SPM voxel-based correlation analysis (mean VOI). To get the validation element of a single PD subject, we repeated the SPM analysis while leaving that specific PD subject out. The new VOI (the significant cluster) was used to extract the mean ^{18}F-FEOBV DVR from that PD subject (mean VOI-LOO). This process was repeated for each of the 45 PD subjects.

To summarize the error between the predicted and observed values for the 2 models, the normalized root-mean-square error was used. Pearson correlation was then used to assess the association of mean QA-LOO and mean VOI-LOO.

Clinical Correlate. To assess the clinical relevance of our main findings, we examined whether the cardinal motor features (subscores of bradykinesia, tremor, rigidity, and postural instability and gait difficulties) and cognitive function (Montreal cognitive assessment score) of PD subjects correlated with the following ratio in the MA hemisphere (a proxy measure of acetylcholine–dopamine imbalance in this hemisphere):

$$\frac{\text{mean } ^{18}\text{F-FEOBV DVR within the putaminal SPM-based VOI}}{\text{mean QA of the nigrostriatal white MA matter tract}}$$

To show the robustness of the dopaminergic PET-informed correlational tractography, we also repeated the previous analyses in this larger sample of PD participants.

Non–voxel-based statistical analyses were performed using STATISTICA software (Stat Soft, Inc., version 8.0). The significance level was set at a P value of less than 0.05. For the correlation tests, we used Pearson correlation for normally distributed variables based on the Shapiro–Wilk test (mean QA [least affected and MA], mean QA-LOO [MA], mean VOI, mean VOI-LOO, imbalance proxy, imbalance proxy LOO, bradykinesia, and tremor subscores); otherwise, we used Spearman correlation. For significant results, we also computed 95% percentile bootstrap CIs.

RESULTS

Association Between Integrity of Dopaminergic Nigrostriatal White Matter Tracts and Striatal Cholinergic Binding in PD Subjects

The mean QA of the MA tract (Fig. 1A) showed a negative correlation with striatal ^{18}F-FEOBV DVR (Fig. 1B), which comprised a cluster in the posterior putamen of the MA hemisphere (P corrected at the cluster level = 0.039; cluster size, 226 voxels; Montreal Neurologic Institute coordinates [x, y, z] of the maximum peak, −27, −9, 11; t value at the peak level, 4.05). Figure 1C shows the negative correlation found between mean QA and mean ^{18}F-FEOBV DVR within the VOI derived from this significant cluster. Figure 1D shows that the mean ^{18}F-FEOBV DVR within that VOI was also significantly higher (9.3%; $P = 0.01$, $t = -2.55$) in the PD group (3.64 ± 0.46) than in the control group (3.33 ± 0.26). The mean QA of the least affected tract showed no significant association.

Levodopa equivalent dose, duration, and stage of disease had no significant effects on these results.

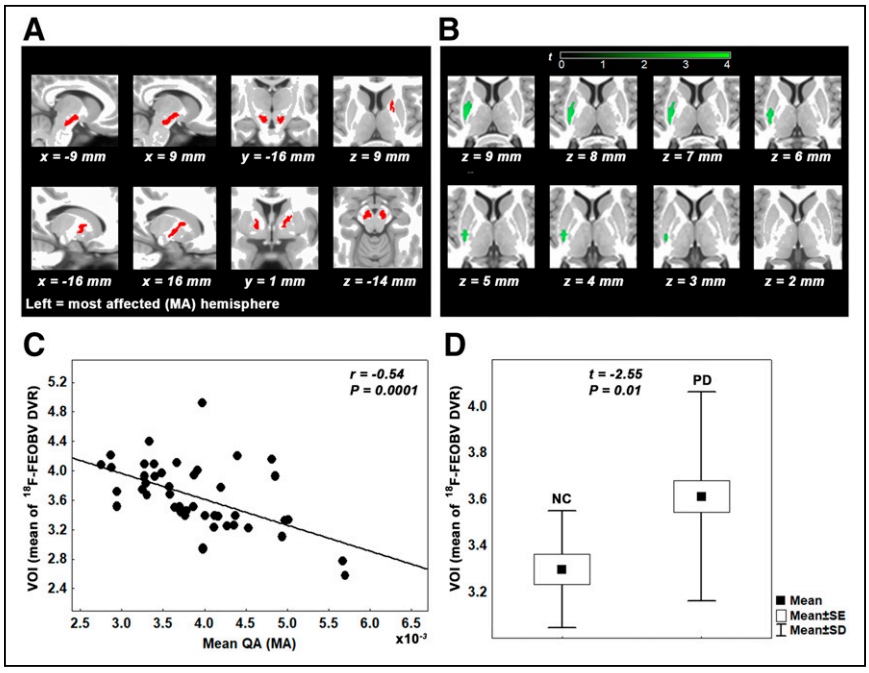

FIGURE 1. (A) Nigrostriatal dopaminergic white matter tracts identified in PD group in MA and least affected hemispheres (overlaid on T1-weighted MR image in Montreal Neurologic Institute space). (B) Voxel-based correlation analysis showing negative correlation between mean QA of MA tract and ^{18}F-FEOBV DVR in posterior putamen of same hemisphere. (C) Negative correlation between mean QA of MA tract and mean ^{18}F-FEOBV DVR within putaminal SPM-based VOI (95% CI, −0.76 to −0.2). (D) Significantly higher mean ^{18}F-FEOBV DVR within that putaminal VOI in PD group than in healthy control (NC) group.

Cross Validation

Figures 2A and 2B show the relationship between predicted and observed values for the MA-tract and VOI models, respectively. The normalized root-mean-square error was 10.36% for the MA-tract model and 4.07% for the VOI model, indicating a lower residual variance for the VOI model. The results of the LOO analysis mirror those of the main analysis. Figure 2C (compare with Fig. 1C) shows a significant negative correlation between the observed mean QA (mean QA-LOO) of the MA tract and the mean ^{18}F-FEOBV DVR within the observed VOI (VOI-LOO). Figure 2D (compare with Fig. 1D) shows that the mean ^{18}F-FEOBV DVR within VOI-LOO was significantly higher ($P = 0.04$, $t = -2.14$) in the PD group (3.58 ± 0.49) than in the control group

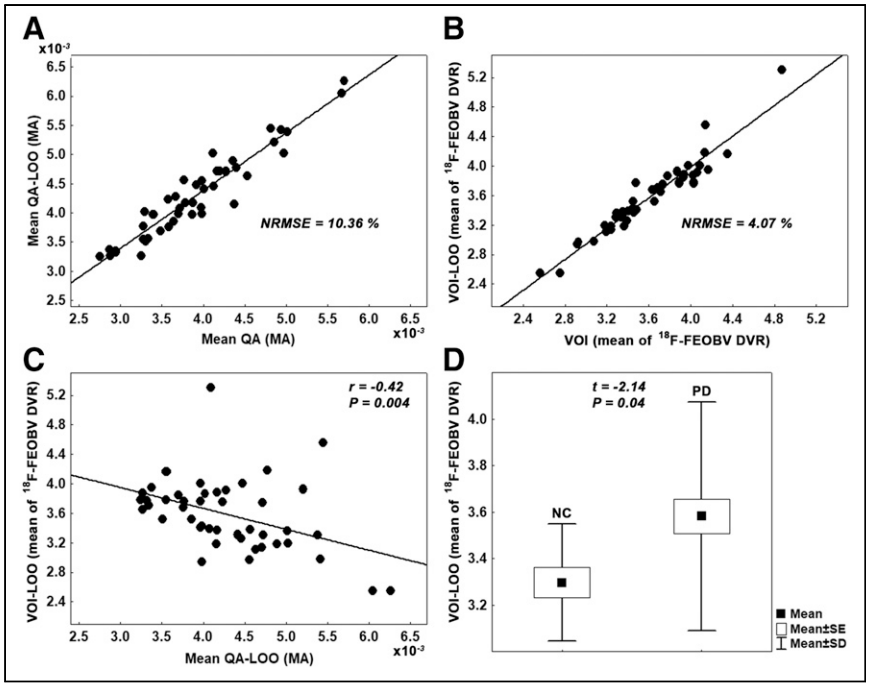

FIGURE 2. (A) Relation between training (predicted values) and cross-validation (observed values) sets using LOO approach (mean QA and mean QA-LOO, respectively) in MA hemisphere of PD subjects. (B) Same as shown in A, but for VOI model derived from SPM voxel-based correlation analysis (VOI and VOI-LOO, respectively). (C) Negative correlation between mean QA-LOO of MA tract and mean ^{18}F-FEOBV DVR within VOI-LOO (95% CI, −0.75 to −0.09). (D) Significantly higher mean ^{18}F-FEOBV DVR within VOI-LOO in PD group than in healthy control (NC) group. NRMSE = normalized root-mean-square error.

(3.33 ± 0.26). These findings cross-validate our observations, suggesting their generalizability to independent datasets of PD subjects with similar clinical characteristics.

Association Between Dopaminergic and Cholinergic Binding at Presynaptic-Terminal Level or Striatal-Terminal Level in PD Subjects

^{11}C-DTBZ DVR for each of the striatal subregions and for the whole striatum showed no significant association with striatal ^{18}F-FEOBV DVR in voxel-based analysis. The same results were found after outlier removal (bilateral putaminal subregions and whole striatum in the MA hemisphere; Supplemental Tables 1 and 2; Supplemental Fig. 1).

To further investigate the association between dopaminergic and cholinergic binding at the presynaptic-terminal level, we performed a post hoc correlation analysis between mean ^{18}F-FEOBV DVR within the significant cluster that correlated with mean QA in the MA hemisphere (Fig. 1B) and the ipsilateral whole striatum ^{11}C DTBZ DVR. The rationale for this post hoc analysis was that whole-striatum ^{11}C DTBZ DVR and mean QA correlate with each other (Supplemental Fig. 2A). The same analysis was performed for ^{11}C-DTBZ DVR in each striatal subregion of that hemisphere. We found that only the whole-striatum ^{11}C DTBZ DVR showed a significant negative correlation (Fig. 3; Supplemental Table 3), although weaker than that observed with the mean QA (Fig. 1C). This correlation remained significant after outlier removal (Supplemental Table 3).

Striatal Cholinergic Binding in PD Group Versus Healthy Control Group

We found a bilateral increase in putaminal ^{18}F-FEOBV DVR in the PD group compared with the control group, more extensive in the MA hemisphere (Fig. 4; Table 2). The maximum peak in each cluster was located in the posterior putamen in each hemisphere. There was a partial overlap with the findings shown in Figure 1B. No significant decrease was found.

Clinical Correlates

Bradykinesia ratings positively correlated with our proxy measure of acetylcholine–dopamine imbalance (Fig. 5A), as well as with the proxy using the measures derived from the LOO analysis (Fig. 5B). Bradykinesia ratings also correlated negatively with the mean QA of the MA tract (Fig. 5C) and positively with the mean ^{18}F-FEOBV DVR within the putaminal VOI (Fig. 5D). The other cardinal motor features and cognitive ratings (Montreal cognitive assessment) did not show significant associations with our proxy measure of imbalance (tremor: $r = -0.08$, $P = 0.6$; rigidity: Spearman $r = 0.13$, $P = 0.4$; postural instability and gait difficulties: Spearman $r = 0.13$, $P = 0.42$; and Montreal cognitive assessment: Spearman $r = 0.01$, $P = 0.9$).

Complementary Findings of Correlational Tractography

Supplemental Figures 2A and 2B show the significant positive correlation found between the mean QA and the striatal ^{11}C-DTBZ DVR in both brain hemispheres. Likewise, the comparison between the 2 hemispheric tracts showed a significant reduction in the mean QA of the MA tract (Supplemental Fig. 2C). The mean QA-LOO in the MA hemisphere also showed a positive correlation with the striatal ^{11}C-DTBZ DVR of that hemisphere (Supplemental Fig. 2D). The nigrostriatal dopaminergic white matter tracts followed anatomic paths similar to those observed in our previous study (*18*).

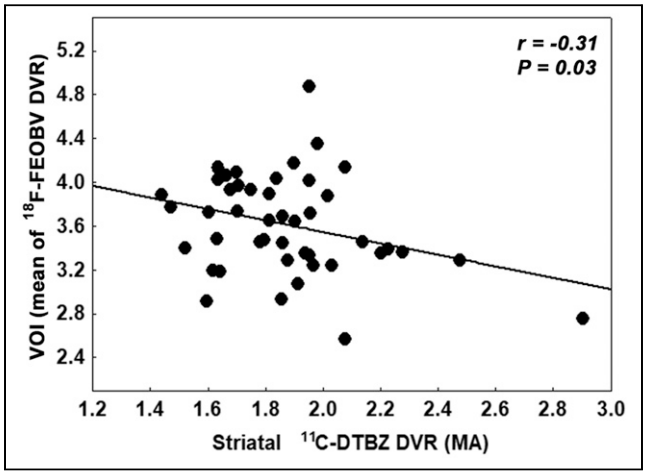

FIGURE 3. Negative correlation between mean ^{18}F-FEOBV DVR within significant cluster correlated with mean QA in MA hemisphere (Fig. 1B) and ipsilateral whole striatum^{11}C-DTBZ DVR (95% CI, −0.55 to −0.02).

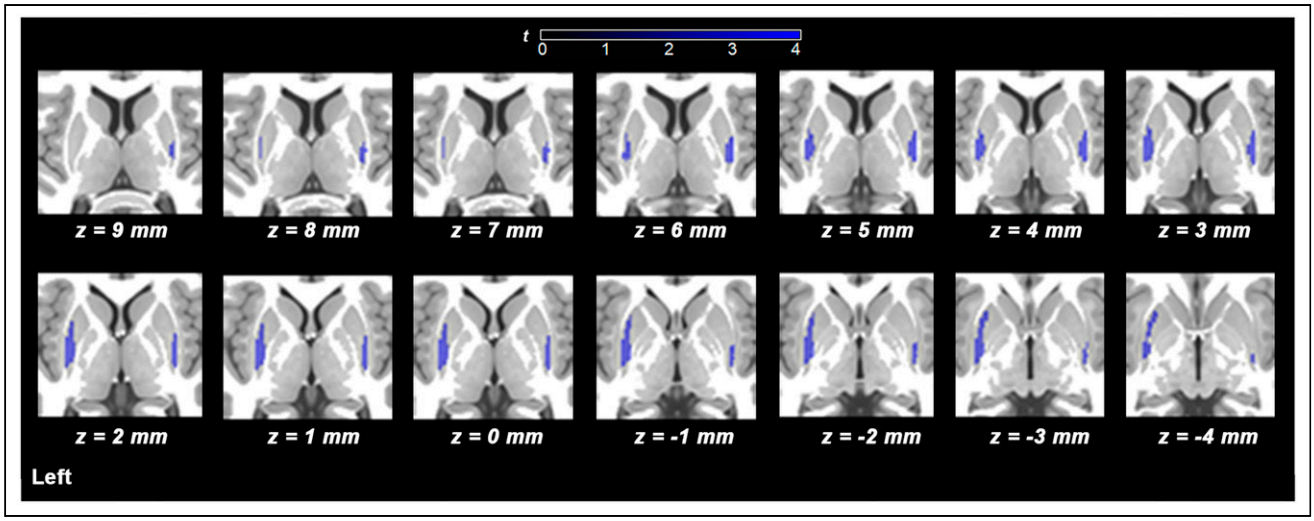

FIGURE 4. Voxel-based group comparison showing asymmetric bilateral putaminal ^{18}F-FEOBV DVR increases (more extensive in MA hemisphere [left]), compared with control group (Table 2). There is partial topographic overlap of MA side with results of voxel-based correlation analysis in PD group (Fig. 1B, z = 6–4 mm [left]).

DISCUSSION

In this study, we examined the striatal acetylcholine–dopamine imbalance hypothesis in patients with early PD. Our results showed an increase in cholinergic binding in the posterior putamen of the MA brain hemisphere, associated with an ipsilateral reduction in the integrity of the nigrostriatal dopaminergic white matter tract in PD patients. In addition, cholinergic binding in this striatal region was increased in PD patients compared with healthy controls. These results were cross-validated. We also showed that bradykinesia clinical subscores positively correlated with a proxy measure of acetylcholine–dopamine imbalance in the MA hemisphere. Taken together, our results provide evidence for the striatal acetylcholine–dopamine imbalance in early PD and may provide an avenue for testing in vivo effects of therapeutic strategies aimed at restoring striatal acetylcholine–dopamine balance in PD.

Our observations are in line with previous studies on animal models of PD showing that reduced striatal dopamine signaling leads to increased excitability and synaptic reorganization of striatal cholinergic interneurons and increased acetylcholine release (*9*).

Our findings suggest that the association between acetylcholine (^{18}F-FEOBV binding) and the integrity loss of the nigrostriatal dopaminergic pathway is stronger and more robust at the level of dopaminergic nigrostriatal connectivity (i.e., loss of mean QA of the nigrostriatal tract, Fig. 1C) than at the presynaptic-terminal level (i.e., loss of striatal ^{11}C-DTBZ binding, Fig. 3). This finding is probably due to several factors: first, ^{11}C-DTBZ binding may underestimate the severity of damage to the nigrostriatal end-terminal in PD because of compensatory changes (*17*). In contrast, the mean QA of the MA hemispheric tract fibers is probably less influenced by the ^{11}C-DTBZ's compensation mechanism. The estimation of the mean QA uses not only the information derived from the ^{11}C-DTBZ PET but also white matter fibers derived from dMRI. Second, striatal neurotransmission involves not only acetylcholine and dopamine but also other extrinsic (e.g., glutamatergic projections from the thalamus and cortex) and intrinsic (e.g., γ-aminobutyric acid–ergic interneurons) determinants, which may have interacting effects with striatal dopaminergic neurons and cholinergic interneurons at the level of presynaptic nerve terminals (*7–9*). In contrast, the dopaminergic nigrostriatal tract includes structural connectivity information specific for dopaminergic neurotransmission and thus less affected by other neurotransmitter interactions. It is also possible that cholinergic upregulation may be more prominent in the prodromal stage but becomes less so in the symptomatic stage of PD, thus diluting the possible one-to-one relationship between striatal acetylcholine and dopamine at the level of presynaptic nerve terminals (*36*). Therefore, the dopaminergic nigrostriatal tract may be a more precise marker of the integrity of the nigral dopaminergic cells than is the more downstream distal degeneration of the nerve terminals. The observed decrease in the tract integrity could be the result of the distal-to-proximal axonal degenerative "dying back" process in PD (*37*).

TABLE 2
Striatal Cholinergic Binding Increase in PD Group Compared with Control Group

Striatal region	*P*	Cluster size	Montreal Neurologic Institute coordinates (*x, y, z*) of maximum peak	Peak-level *t* value
MA putamen	0.028	369 voxels	−32, −8, 5	3.93
Least affected putamen	0.043	188 voxels	32, −9, 6	4.15

P value is corrected for multiple comparisons at cluster level by using familywise error approach.

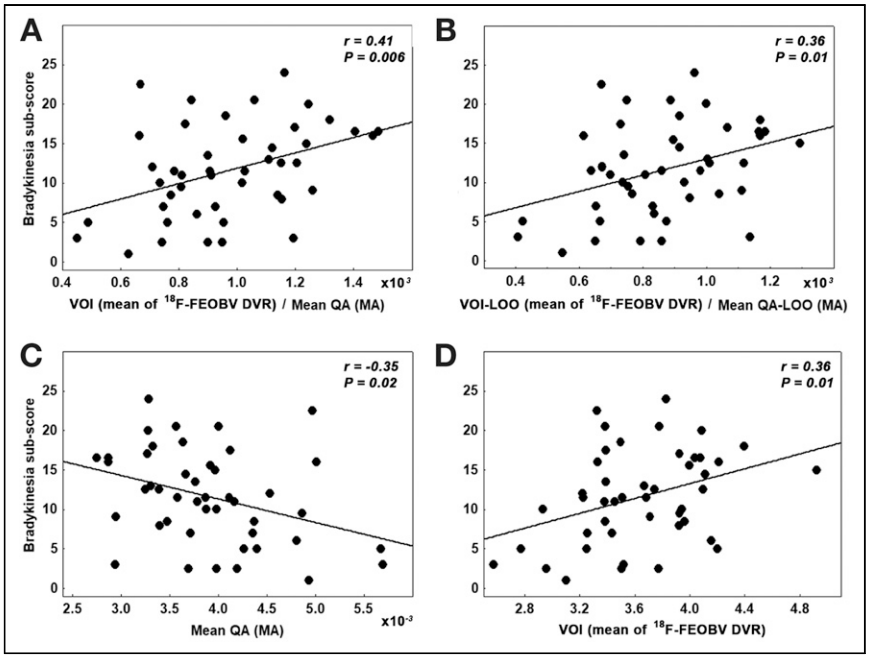

FIGURE 5. (A) Positive correlation between bradykinesia subscore and proxy measure of acetylcholine–dopamine imbalance in MA hemisphere in subjects with PD (95% CI, 0.15–0.62). (B) Same as shown in A, but using measures derived from LOO cross-validation analysis (95% CI, 0.07–0.59). (C) Negative correlation between bradykinesia subscore and mean QA in MA hemisphere (95% CI, −0.63 to −0.01). (D) Positive correlation between bradykinesia subscore and mean ^{18}F-FEOBV DVR within putaminal SPM-based VOI in MA hemisphere (95% CI, 0.1–0.58).

Our proxy measure for acetylcholine–dopamine imbalance was positively correlated with clinical bradykinesia ratings. This finding may be explained by the fact that bradykinesia has a closer association with striatal dopaminergic activity than do the other cardinal motor symptoms (*38*). This observation also agrees with a previous study on a PD mouse model showing that photoinhibition of striatal cholinergic interneurons reduces bradykinesia (*39*). Other cardinal symptoms and cognitive function did not show an association with our imbalance proxy. These other impairments are likely caused by more expanded brain networks that extend beyond the striatum (*40–42*). Our study focused only on the striatum to reduce the complexity of the acetylcholine–dopamine interactions and to be consistent with the existing literature on the acetylcholine–dopamine imbalance in PD.

The discrepant findings between some previous animal studies (*10–12*) and our current in vivo human PD results may be related to differences between the generally more uniform toxic or lesioning animal PD models and the natural history of the insidious and long duration of dopaminergic degeneration, as well as interindividual variability in patients with PD. Moreover, our presynaptic vesicular transporter PET measures may reflect a more relative steady state of the integrity of nerve terminals rather than the typical more dynamic signaling changes observed in animal models.

A strength of this study was the use of ^{11}C-DTBZ PET–informed correlational tractography (*18*). We also replicated and extended this methodology in a larger sample of patients with early PD. Unlike our previous study, we were able to also cross-validate the tract in the MA hemisphere, probably because of the larger sample that allowed a more robust estimate of the tract template in that hemisphere.

Our study had several limitations. First, dopaminergic PET was performed in the dopaminergic medication–off state, whereas cholinergic PET was performed on dopaminergic medications. Nevertheless, it is possible that the imbalance between the acetylcholine and dopamine markers would have been even greater than that observed in this study if both PET scans had been performed in the off state. Second, our study was cross sectional, preventing us from evaluating the evolution of the acetylcholine–dopamine interaction in PD over time. Third, the effect of sex or clinical phenotype on the acetylcholine–dopamine interaction was not assessed, as larger samples of PD subjects would be needed for this purpose. Fourth, we were unable to investigate the acetylcholine–dopamine interaction in healthy controls because of the lack of ^{11}C-DTBZ PET in these subjects. However, a lower putaminal ^{18}F-FEOBV DVR found in healthy controls than in PD patients may be consistent with the prevailing view that acetylcholine and dopamine are balanced in healthy conditions. Other limitations were related to the methodology for estimating the nigrostriatal dopaminergic tracts (*18*). For example, we cannot rule out that the identified tracts also included some nondopaminergic fibers, and the identified tracts extended slightly below the substantia nigra, as may be due to limitations in the spatial resolution of dMRI. Nonetheless, the use of ^{11}C-DTBZ PET–informed correlational tractography has higher dopaminergic specificity than does tract definition using dMRI alone. Finally, future neuroimaging studies should take into account more expanded brain networks and other key players that could shed more light on the complexity of acetylcholine–dopamine interaction (e.g., dopaminergic and cholinergic receptors as well as other neurotransmitters).

CONCLUSION

Using dual-tracer PET and dopaminergic PET–informed correlational tractography, we provided in vivo evidence of imbalance between acetylcholine and dopamine signaling systems in the striatum in early PD. These observations may provide a future avenue for testing in vivo effects of therapeutic strategies aimed at restoring striatal acetylcholine–dopamine balance in PD.

DISCLOSURE

Funding was received from the NIH, the Department of Veterans Affairs, and the Michael J. Fox Foundation. No other potential conflict of interest relevant to this article was reported.

ACKNOWLEDGMENTS

We thank Christine Minderovic, Cyrus Sarosh, Jacqueline Dobson, the PET technologists, the cyclotron operators, the radiochemists, and, especially, our patients with PD and our research volunteers.

KEY POINTS

QUESTION: Is there an imbalance between the acetylcholine and dopamine signaling systems in the striatum in early PD?

PERTINENT FINDINGS: In a cohort study using cholinergic and dopaminergic PET and correlational tractography, an imbalance was found between the acetylcholine and dopamine signaling systems in the striatum of 45 patients with mild to moderate PD. This imbalance was evidenced by an increase in cholinergic binding in the posterior putamen in the MA brain hemisphere—an increase that correlated with the ipsilateral reduction in the integrity of the dopaminergic nigrostriatal white matter tract and clinically with more severe bradykinesia.

IMPLICATIONS FOR PATIENT CARE: Assessment of the striatal acetylcholine–dopamine imbalance may provide a method for in vivo testing of the effects of therapeutic strategies aimed at reducing this imbalance in early PD.

REFERENCES

1. Mesulam MM, Mash D, Hersh L, Bothwell M, Geula C. Cholinergic innervation of the human striatum, globus pallidus, subthalamic nucleus, substantia nigra, and red nucleus. *J Comp Neurol.* 1992;323:252–268.
2. Bolam JP, Wainer BH, Smith AD. Characterization of cholinergic neurons in the rat neostriatum: a combination of choline acetyltransferase immunocytochemistry, Golgi-impregnation and electron microscopy. *Neuroscience.* 1984; 12:711–718.
3. Barbeau A. The pathogenesis of Parkinson's disease: a new hypothesis. *Can Med Assoc J.* 1962;87:802–807.
4. Aosaki T, Miura M, Suzuki T, Nishimura K, Masuda M. Acetylcholine-dopamine balance hypothesis in the striatum: an update. *Geriatr Gerontol Int.* 2010;10(suppl 1): S148–S157.
5. Lang AE, Lozano AM. Parkinson's disease: second of two parts. *N Engl J Med.* 1998;339:1130–1143.
6. Bridi JC, Hirth F. Mechanisms of α-synuclein induced synaptopathy in Parkinson's disease. *Front Neurosci.* 2018;12:80.
7. Girasole AE, Nelson AB. Probing striatal microcircuitry to understand the functional role of cholinergic interneurons. *Mov Disord.* 2015;30:1306–1318.
8. Tanimura A, Pancani T, Lim SAO, et al. Striatal cholinergic interneurons and Parkinson's disease. *Eur J Neurosci.* 2018;47:1148–1158.
9. Ztaou S, Amalric M. Contribution of cholinergic interneurons to striatal pathophysiology in Parkinson's disease. *Neurochem Int.* 2019;126:1–10.
10. Herrera-Marschitz M, Goiny M, Utsumi H, et al. Effect of unilateral nucleus basalis lesion on cortical and striatal acetylcholine and dopamine release monitored in vivo with microdialysis. *Neurosci Lett.* 1990;110:172–179.
11. Herrera-Marschitz M, Luthman J, Ferre S. Unilateral neonatal intracerebroventricular 6-hydroxydopamine administration in rats: II. Effects on extracellular monoamine, acetylcholine and adenosine levels monitored with in vivo microdialysis. *Psychopharmacology (Berlin).* 1994;116:451–456.
12. McKinley JW, Shi ZQ, Kawikova I, et al. Dopamine deficiency reduces striatal cholinergic interneuron function in models of Parkinson's disease. *Neuron.* 2019; 103:1056–1072.e6.
13. Petrou M, Frey KA, Kilbourn MR, et al. In vivo imaging of human cholinergic nerve terminals with (−)-5-^{18}F-fluoroethoxybenzovesamicol: biodistribution, dosimetry, and tracer kinetic analyses. *J Nucl Med.* 2014;55:396–404.
14. Bohnen NI, Albin RL, Koeppe RA, et al. Positron emission tomography of monoaminergic vesicular binding in aging and Parkinson disease. *J Cereb Blood Flow Metab.* 2006;26:1198–1212.
15. Perlmutter JS, Norris SA. Neuroimaging biomarkers for Parkinson disease: facts and fantasy. *Ann Neurol.* 2014;76:769–783.
16. de la Fuente-Fernández R. Imaging of dopamine in PD and implications for motor and neuropsychiatric manifestations of PD. *Front Neurol.* 2013;4:90.
17. de la Fuente-Fernández R, Sossi V, McCormick S, Schulzer M, Ruth TJ, Stoessl AJ. Visualizing vesicular dopamine dynamics in Parkinson's disease. *Synapse.* 2009;63:713–716.
18. Sanchez-Catasus CA, Bohnen NI, Yeh FC, D'Cruz N, Kanel P, Müller MLTM. Dopaminergic nigrostriatal connectivity in early Parkinson disease: in vivo neuroimaging study of ^{11}C-DTBZ PET combined with correlational tractography. *J Nucl Med.* 2021;62: 545–552.
19. Yeh FC, Tseng WY. NTU-90: a high angular resolution brain atlas constructed by q-space diffeomorphic reconstruction. *Neuroimage.* 2011;58:91–99.
20. Zhang H, Wang Y, Lu T, et al. Differences between generalized q-sampling imaging and diffusion tensor imaging in the preoperative visualization of the nerve fiber tracts within peritumoral edema in brain. *Neurosurgery.* 2013;73:1044–1053.
21. Yeh FC, Vettel JM, Singh A, et al. Quantifying differences and similarities in whole-brain white matter architecture using local connectome fingerprints. *PLOS Comput Biol.* 2016;12:e1005203.
22. Hughes AJ, Daniel SE, Kilford L, Lees AJ. Accuracy of clinical diagnosis of idiopathic Parkinson's disease: a clinico-pathological study of 100 cases. *J Neurol Neurosurg Psychiatry.* 1992;55:181–184.
23. Goetz CG, Fahn S, Martinez-Martin P, et al. Movement Disorder Society-sponsored revision of the unified Parkinson's disease rating scale (MDS-UPDRS): process, format, and clinimetric testing plan. *Mov Disord.* 2007;22:41–47.
24. Hoehn MM, Yahr MD. Parkinsonism: onset, progression and mortality. *Neurology.* 1967;17:427–442.
25. Nasreddine ZS, Phillips NA, Bedirian V, et al. The Montreal cognitive assessment, MoCA: a brief screening tool for mild cognitive impairment. *J Am Geriatr Soc.* 2005;53:695–699.
26. Müller ML, Albin RL, Kotagal V, et al. Thalamic cholinergic innervation and postural sensory integration function in Parkinson's disease. *Brain.* 2013;136:3282–3289.
27. Bohnen NI, Kanel P, Zhou Z, et al. Cholinergic system changes of falls and freezing of gait in Parkinson disease. *Ann Neurol.* 2019;85:538–549.
28. Jewett DM, Kilbourn MR, Lee LC. A simple synthesis of [^{11}C] dihydrotetrabenazine (DTBZ). *Nucl Med Biol.* 1997;24:197–199.
29. Shao X, Hoareau R, Hockley BG, et al. Highlighting the versatility of the Tracerlab synthesis modules. Part 1: fully automated production of [^{18}F]labelled radiopharmaceuticals using a Tracerlab FX_{FN}. *J Labelled Comp Radiopharm.* 2011;54:292–307.
30. Minoshima S, Frey KA, Koeppe RA, Foster NL, Kuhl DE. A diagnostic approach in Alzheimer's disease using three-dimensional stereotactic surface projections of fluorine-18-FDG PET. *J Nucl Med.* 1995;36:1238–1248.
31. Logan J, Fowler JS, Volkow ND, Wang GJ, Ding YS, Alexoff DL. Distribution volume ratios without blood sampling from graphical analysis of PET data. *J Cereb Blood Flow Metab.* 1996;16:834–840.
32. Nejad-Davarani S, Koeppe RA, Albin RL, Frey KA, Muller M, Bohnen NI. Quantification of brain cholinergic denervation in dementia with Lewy bodies using PET imaging with [^{18}F]-FEOBV. *Mol Psychiatry.* 2019;24:322–327.
33. Kwak Y, Bohnen NI, Müller MLTM, Dayalu P, Seidler RD. Striatal denervation pattern predicts levodopa effects on sequence learning in Parkinson's disease. *J Mot Behav.* 2013;45:423–429.
34. Yeh FC, Wedeen VJ, Tseng WY. Generalized q-sampling imaging. *IEEE Trans Med Imaging.* 2010;29:1626–1635.
35. Yeh FC, Verstynen TD, Wang Y, Fernández-Miranda JC, Tseng WY. Deterministic diffusion fiber tracking improved by quantitative anisotropy. *PLoS One.* 2013;8: e80713.
36. Liu S-Y, Wile DJ, Fu J, et al. The influence of LRRK2 mutations on the cholinergic system in manifest and prodromal stages of Parkinson's disease: a cross-sectional PET study. *Lancet Neurol.* 2018;17:309–316.
37. Tagliaferro P, Burke RE. Retrograde axonal degeneration in Parkinson disease. *J Parkinsons Dis.* 2016;6:1–15.
38. Vingerhoets FJ, Schulzer M, Calne DB, Snow BJ. Which clinical sign of Parkinson's disease best reflects the nigrostriatal lesion? *Ann Neurol.* 1997;41:58–64.
39. Ztaou S, Maurice N, Camon J, et al. Involvement of striatal cholinergic interneurons and M1 and M4 muscarinic receptors in motor symptoms of Parkinson's disease. *J Neurosci.* 2016;36:9161–9172.
40. Dirkx MF, den Ouden H, Aarts E, et al. The cerebral network of Parkinson's tremor: an effective connectivity fMRI study. *J Neurosci.* 2016;36:5362–5372.
41. Baradaran N, Tan SN, Liu A, et al. Parkinson's disease rigidity: relation to brain connectivity and motor performance. *Front Neurol.* 2013;4:67.
42. Kehagia AA, Barker RA, Robbins TW. Cognitive impairment in Parkinson's disease: the dual syndrome hypothesis. *Neurodegener Dis.* 2013;11:79–92.